Manifestation of Weak Localization and Long-Range Correlation in Disordered Wave Functions from Conical Second Harmonic Generation

Y. F. Chen,* K. W. Su, T. H. Lu, and K. F. Huang

Department of Electrophysics, National Chiao Tung University, Hsinchu, Taiwan

(Received 3 November 2005; published 26 January 2006)

We experimentally demonstrate that the near-field patterns of conical second harmonic generation of a laser in random domain structures can be used to explore the spatial structure of two-dimensional disordered wave functions with weak localization. The statistics of the experimental near-field patterns agree very well with the theoretical distributions. In addition to the short-range correlation, the localization effects are found to contribute a nearly constant value to the long-range correlation. The result of this Letter also confirms the possibility of using conical second harmonic generation as a diagnostic tool for topographical characterization of crystals.

DOI: 10.1103/PhysRevLett.96.033905 PACS numbers: 42.25.Dd, 42.55.Xi, 42.65.Ky, 72.15.Rn

Interference effects between scattered waves lead to striking phenomena beyond the radiative transfer treatment and diffusion theory [1]. Weak localization (WL) is a hallmark of interference of multiply scattered waves in disordered media [2–4] and is a direct consequence of the constructive interference between reciprocal paths in wave scattering [5]. The phenomenon of weak localization has been extensively studied in coherent backscattering from colloidal suspension [6], strongly scattering powders [7], cold atom gases [8], two-dimensional (2D) random systems [9], randomized laser materials [10], disordered liquid crystals [11], and disordered microcavities [12]. Especially, microwave experiments have provided direct observation of quantum wave functions in disordered quantum billiards [13]. Even so, there have been few experimental studies of quantum disordered wave functions because of their lack of accessibility.

The underlying wave nature of the particles leads to the striking feature that the propagation of electrons in conducting devices shows many similarities with random multiple scattering of light in disordered media [2–4]. This relevance stimulated active research in the propagation of light waves in random scattering media since the 1980s [6]. Recently, it has been observed that multiple scattering of laser light in a microdomained nonlinear crystal constitutes a novel mechanism for conical second harmonic generation (SHG) [14]. The coherent wave in laser cavities enables one to achieve very precise measurements of intensity patterns. Nevertheless, experiments on the spatial structure of disordered wave functions with conical SHG have never been realized as yet.

In this Letter, we originally develop an intracavity conical SHG scheme to explore the spatial structure of 2D disordered wave functions with weak localization. By using a nonlinear crystal with extended defects, the conical SHG is efficiently produced from a Q-switched laser with intracavity frequency doubling. The near-field patterns of the conical SHG beams evidently represent the wave functions of disordered quantum systems. The statistics of the wave functions are found to be in quantitative agreement with the supersymmetry sigma model [15]. More importantly, the analysis of the intensity correlation for the experimental patterns reveals that the localization effects significantly enhance the magnitude of the long-range correlation.

In the past few years, a new nonlinear crystal family of calcium oxyborates such as $GdCa_4O(BO_3)_3$ (GdCOB) and $YCa_4O(BO_3)_3$ has been developed for efficient SHG and other parametric processes in various fields [16]. The optical properties of the nonlinear crystals are greatly affected by their structural imperfection that is strongly dependent on the material preparation and the growth conditions. Recent investigations [17] revealed that the disordered domain structures may be spontaneously present in nominal GdCOB samples which do not contain any macroscopic defects and cracks. Intriguingly, the presence of an appropriate distribution of disordered domains allows broadband frequency conversion processes without any temperature or angular tuning of the crystal, especially for conical SHG. Here we used a GdCOB crystal with moderate random defect domains to investigate the spatial structure of disordered wave functions. Figure 1 depicts the experimental configuration for the diode-pumped actively Q-switched Nd:YAG laser with intracavity SHG in the GdCOB crystal. The input mirror is a 500 mm radius-of-curvature concave mirror with antireflection coating at 808 nm on the entrance face ($R < 0.2\%$), high-reflection coating at 1064 nm ($R > 99.8\%$) and 532 nm ($R > 99\%$), and high-transmission coating at 808 nm on the other surface ($T > 90\%$). The output coupler is a flat mirror with high-reflection coating at 1064 nm ($R > 99.8\%$) and high-transmission coating at 532 nm ($T > 85\%$). The pump source was an 808 nm fiber-coupled laser diode with a core diameter of 800 μm, a numerical aperture of 0.16, and a maximum output power of 10 W. A focusing lens with 12.5 m focal length and 90% coupling efficiency

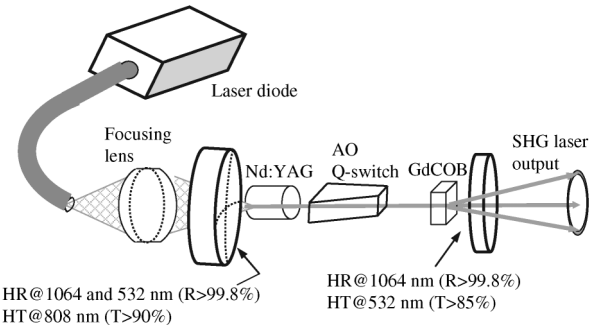

FIG. 1. The experimental configuration for the diode-pumped actively Q-switched Nd:YAG laser with intracavity SHG in the GdCOB crystal.

was used to reimage the pump beam into the laser crystal. The laser medium was a 0.8-at. % Nd^{3+}:YAG crystal with a length of 10 mm. The GdCOB crystal was cut for type I frequency doubling in the XY planes ($\theta = 90°$, $\phi = 46°$) with a length of 2 mm and a cross section of 3 mm $\times$ 3 mm. Both sides of the Nd:YAG and GdCOB crystals were coated for antireflection at 1064 nm ($R < 0.2\%$). The diameters of the laser beams were approximately 580 and 500 μm in the Nd:YAG and GdCOB crystals, respectively. The 30 mm-long acousto-optic Q switch (NEOS Technologies) had antireflection coatings at 1064 nm on both faces and was driven at a 27.12 MHz center frequency with 15.0 W of rf power. The laser cavity length was approximately 10 cm.

The pulse repetition rate for the Q-switched pulses was fixed at 20 kHz. The lasing thresholds for the axial and conical SHG beams were nearly the same and approximately 3 W. The typical far-field pattern is shown in Fig. 2(a). At a pump power of 8 W, the output powers of both the axial and conical SHG beams were on the order of 1 mW. The phase-matching condition for the conical SHG in a nonlinear crystal with disordered domain structures is generally written as $\bar{k}_1 + \bar{k}_1' = \bar{k}_2$, as shown in Fig. 2(b), where $\bar{k}_1$ is the axial fundamental beam, $\bar{k}_1'$ is the scattered off-axis fundamental beam, and $\bar{k}_2$ is the phase-matched off-axis SHG beam. The cone angle φ is determined by the effective refractive indices. Experimental results revealed that the cone angles of the far-field patterns were almost the same for all the transverse positions of the GdCOB crystal. Even so, the near-field patterns were found to be profoundly related to the topographical characterization of the nonlinear crystal. Figures 3(a)–3(d) show four examples of the near-field wave patterns measured at different transverse positions of the GdCOB crystal. It can be seen that the experimental near-field pattern $|\Psi(\bar{r})|^2$ exhibits a network of quasilinear ridge structures which result from the superposition of monochromatic plane waves with random directions and phases in two dimensions, as discovered by O'Connor, Gehlen, and Heller [18]. Note that the paraxial propagation and the phase-matching condition lead the present conical SHG to be a kind of 2D random scattering process. The quasilinear ridge patterns should be distinguished from the ordinary speckle patterns that are a 2D projection of the light formed by the superposition of monochromatic plane waves with random directions and phases in three dimensions. In other words, the ordinary speckle pattern has a spread in the magnitudes of the projected wave vectors, whereas the quasilinear ridge pattern consists of only a nearly constant transverse wave vector. With the cone angle of the far-field patterns, the present near-field patterns are associated with a superposition of random plane waves with the transverse wave number $K = k_2 \sin\varphi$. To our knowledge, this is the first time that the near-field patterns of conical SHG are used to visualize the spatial structures of the quantum disordered wave functions.

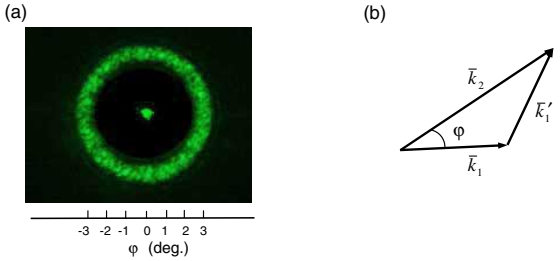

FIG. 2 (color online). (a) The typical far-field pattern of conical SHG. (b) Phase-matching diagram for a conical SHG process in which $\bar{k}_1$ is the axial fundamental beam, $\bar{k}_1'$ is the scattered off-axis fundamental beam, and $\bar{k}_2$ is the phase-matched off-axis SHG beam.

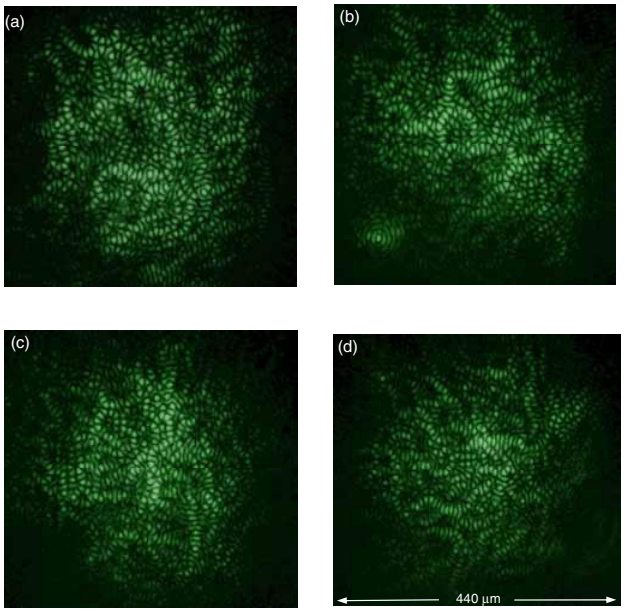

FIG. 3 (color online). Four examples of the near-field wave patterns measured at different transverse positions of the GdCOB crystal.

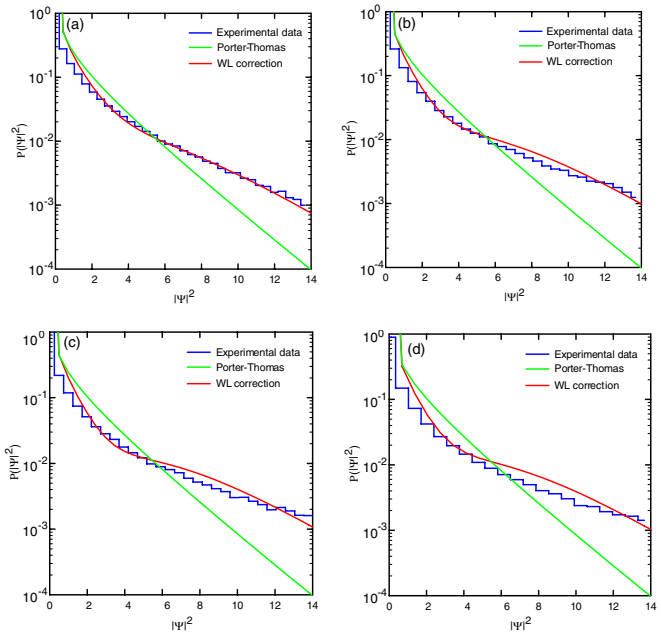

FIG. 4 (color online). (a)–(d) The density probabilities $P(I)$ for the experimental data shown in Figs. 3(a)–3(d), respectively.

The density probability distribution $P(I)$ is extensively used to characterize the localization of the wave function, where $I = |\Psi|^2$. Fyodorov and Mirlin [15] found that the density probability distribution for the normalized disordered wave functions with WL can be expressed as

$$P_{\mathrm{FM}}(I) = P_{\mathrm{PT}}(I)[1 + (\mathrm{IPR} - 3)(\tfrac{1}{8} - \tfrac{1}{4}I + \tfrac{1}{24}I^2)], \quad (1)$$

where $P_{\mathrm{PT}}(I) = \exp(-I/2)/\sqrt{2\pi I}$ is the classic Porter-Thomas (PT) distribution, and $\mathrm{IPR} = \int I^2 d^2 r$ is the inverse participation ratio that is closely linked to the degree of localization. The IPR for chaotic systems can be immediately obtained from PT distribution, i.e., $\mathrm{IPR} = \int_0^\infty I^2 P_{\mathrm{PT}}(I) dI = 3.0$, which is a universal value. The IPR is inversely proportional to the volume in which the wave function is confined. As a consequence, the IPR values for disordered systems are generally greater than 3.0, and large IPR values correspond to strongly localized states. We analyzed the experimental near-field patterns to obtain the density probability distribution. Figures 4(a)–4(d) display the density probabilities $P(I)$ for the experimental data shown in Figs. 3(a)–3(d), respectively. The IPR values for the experimental wave patterns in Figs. 3(a)–3(d) are 4.39, 4.91, 5.35, and 5.67, respectively. All four intensity distributions clearly deviate from the PT distribution but show fairly good agreement with the theoretical distribution $P_{\mathrm{FM}}(I)$. The good agreement indicates that the localization effect plays an important role for conical SHG in disordered domain structures.

With the experimental near-field patterns, we calculated the intensity correlation function (ICF) to get further information about the disordered wave function. The ICF for

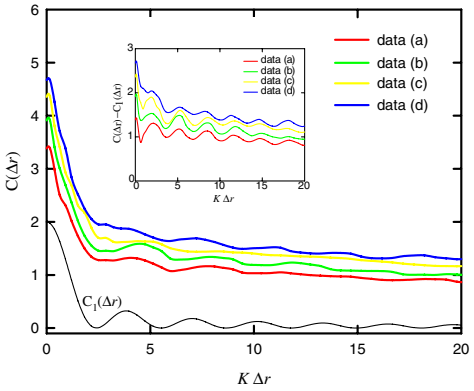

FIG. 5 (color online). The measurement of intensity correlation function $C(\Delta r)$ for the experimental wave patterns shown in Figs. 3(a)–3(d). Inset: The difference $C(\Delta r) - C_1(\Delta r)$.

the normalized wave function is defined as $C(\Delta r) = \langle (I(\bar{r})I(\bar{r}')\rangle - 1$, where $\Delta r = |\bar{r} - \bar{r}'|$. The ICF $C(\Delta r)$ for disorder systems is composed of three terms describing short-range $C_1(\Delta r)$, long-range $C_2(\Delta r)$, and infinite-range $C_3(\Delta r)$ [19]. For the 2D orthogonal case, $C_1(\Delta r)$ is given by $2J_0(K\Delta r)$, where J_0 is the Bessel function of zero order. Note that the ICF for chaotic systems is contributed only by $C_1(\Delta r)$. Figure 5 shows the measurement of $C(\Delta r)$ for the experimental wave patterns shown in Figs. 3(a)–3(d). Since $C(\Delta r)$ at $\Delta r = 0$ is equal to the value of (IPR − 1), the increase of the short-range correlation due to localization is perceptible. A more intriguing feature is that the measured $C(\Delta r)$ are found to approach a constant value for long range. The spatial dependence of the long-range contribution can be examined from the difference $C(\Delta r) - C_1(\Delta r)$, as shown in the inset in Fig. 5. It can be seen that the long-range contribution depends on the degree of localization, and its magnitude increases with increasing the IPR value. The similar long-range correlation has also been observed in the transmission of microwaves [20]. Although numerical study of light in a random medium reveals the analogous phenomenon [21], the present investigation provides the first experimental evidence for the long-range correlation due to transverse localization.

In summary, the spatial structure of 2D disorder wave functions with weak localization has been explored with the conical SHG of a laser in random domain structures. The statistics of the experimental near-field patterns are found to be in quantitative agreement with the theoretical distributions with the correction of weak localization. Furthermore, the analysis of the ICF reveals that the localization effect not only increases the magnitude of the short-range correlation but also introduces a nearly constant value to the long-range correlation. The present result also confirms the possibility of using conical SHG as a diagnostic tool for topographical characterization of crystals in which localization phenomenon occurs naturally.

This work is supported by the National Science Council of Taiwan (Contract No. NSC-94-2112-M-009-034).

*Electronic address: yfchen@cc.netu.edu.tw

[1] E. Abrahams, P. W. Anderson, D. C. Licciardello, and T. V. Ramakrishnan, Phys. Rev. Lett. **42**, 673 (1979); S. John, Phys. Rev. Lett. **53**, 2169 (1984); P. W. Anderson, Philos. Mag. B **52**, 505 (1985); F. Scheffold and G. Maret, Phys. Rev. Lett. **81**, 5800 (1998).

[2] P. Sheng, *Introduction to Wave Scattering, Localization, and Mesoscopic Phenomena* (Academic, New York, 1995).

[3] V. L. Kuzmin and V. P. Romanov, Phys. Usp. **39**, 231 (1996).

[4] M. C. W. van Rossum and Th. M. Nieuwenhuizen, Rev. Mod. Phys. **71**, 313 (1999).

[5] B. A. van Tiggelen, Phys. Rev. Lett. **75**, 422 (1995); B. A. van Tiggelen and R. Maynard, in *Wave Propagation in Complex Media*, edited by G. Papanicolaou, IMA Volumes in Mathematics and Its Applications Vol. 96 (Springer, New York, 1998).

[6] M. P. van Albada and A. Lagendijk, Phys. Rev. Lett. **55**, 2692 (1985); P. E. Wolf and G. Maret, Phys. Rev. Lett. **55**, 2696 (1985).

[7] D. S. Wiersma, M. P. van Albada, B. A. Van Tiggelen, and A. Lagendijk, Phys. Rev. Lett. **74**, 4193 (1995).

[8] G. Labeyrie, F. De Tomasi, J. C. Bernard, C. A. Müller, C. Miniatura, and R. Kaiser, Phys. Rev. Lett. **83**, 5266 (1999); Y. Bidel, B. Klappauf, J. C. Bernard, D. Delande, G. Labeyrie, C. Miniatura, D. Wilkowski, and R. Kaiser, Phys. Rev. Lett. **88**, 203902 (2002).

[9] I. Freund, M. Rosenbluh, R. Berkovitsm, and M. Kaveh, Phys. Rev. Lett. **61**, 1214 (1988).

[10] D. S. Wiersma, M. P. van Albada, and A. Lagendijk, Phys. Rev. Lett. **75**, 1739 (1995).

[11] R. Sapienza, S. Mujumdar, C. Cheung, A. G. Yodh, and D. Wiersma, Phys. Rev. Lett. **92**, 033903 (2004); L. V. Kuzmin, V. P. Romanov, and L. A. Zubkov, Phys. Rev. E **54**, 6798 (1996).

[12] M. Gurioli, F. Bogani, L. Cavigli, H. Gibbs, G. Khitrova, and D. S. Wiersma, Phys. Rev. Lett. **94**, 183901 (2005).

[13] P. Pradhan and S. Sridhar, Phys. Rev. Lett. **85**, 2360 (2000); A. Kudrolli, V. Kidambi, and S. Sridhar, Phys. Rev. Lett. **75**, 822 (1995); M. Barth, U. Kuhl, and H. J. Stöckmann, Phys. Rev. Lett. **82**, 2026 (1999).

[14] A. R. Tunyagi, M. Ulex, and K. Betzler, Phys. Rev. Lett. **90**, 243901 (2003); P. Xu, S. H. Ji, S. N. Zhu, X. Q. Yu, J. Sun, H. T. Wang, J. L. He, Y. Y. Zhu, and N. B. Ming, Phys. Rev. Lett. **93**, 133904 (2004).

[15] Y. V. Fyodorov and A. D. Mirlin, Phys. Rev. B **51**, 13 403 (1995); A. D. Mirlin, Phys. Rep. **326**, 259 (2000); V. Prigodin and B. Altshuler, Phys. Rev. Lett. **80**, 1944 (1998); K. B. Efetov, *Supersymmetry in Disorder and Chaos* (Cambridge University Press, Cambridge, England, 1997).

[16] M. V. Pack, D. J. Armstrong, A. V. Smith, G. Aka, B. Ferrand, and D. Pelenc, J. Opt. Soc. Am. B **22**, 417 (2005).

[17] M. Lefeld-Sosnowska, E. Olszyńska, A. Pajaczkowska, and A. Klos, J. Cryst. Growth **262**, 388 (2004).

[18] P. O'Connor, J. Gehlen, and E. J. Heller, Phys. Rev. Lett. **58**, 1296 (1987).

[19] S. Feng, C. Kane, P. A. Lee, and A. D. Stone, Phys. Rev. Lett. **61**, 834 (1988).

[20] P. Sebbah, B. Hu, A. Z. Genack, R. Pnini, and B. Shapiro, Phys. Rev. Lett. **88**, 123901 (2002).

[21] S. H. Chang, A. Taflove, A. Yamilov, A. Burin, and H. Cao, Opt. Lett. **29**, 917 (2004).